JOC The Journal of Organic Chemistry

pubs.acs.org/joc Article

Computational Exploration of Anomalous Regioselectivities in Cycloadditions of Ketenes to Oxazolines

Ledong Zhu Mark A. Maskeri Melissa Ramirez F. Le Bideau Léon Ghosez and K. N. Houk

Cite This: J Org Chem 2022 87 3613 3622 Read Online

CCESS | Metrics More | Article Recommendations | Supporting Information

ABSTRACT: Thermal (2 + 2) cycloadditions of several *N*-carboalkoxy (*R*)-2-*tert*-butyldihydrooxazoles with ketenes have been studied experimentally by the Ghosez group. Contrary to results from Seebach and co-workers that the electrophilic addition of acylating agents occurs to dihydrooxazole nitrogen, Ghosez found major cycloadducts resulting from an attack of ketene carbonyl carbon to oxygen. We investigate the potential energy surface for the cycloaddition of diphenyl- and phenylchloroketenes to two (*R*)-2-*tert*-butyldihydrooxazoles with ωB97X-D and mPW1PW91 density functional theory and DLPNO-CCSD(T) wave function theory. These (2 + 2) cycloadditions are concerted but highly asynchronous, and the selectivity trends in ketene addition cases are in good agreement with the experiment. We propose a model based on the buildup of charge in oxazoline to reconcile the regiochemical di erences between Ghosez and Seebach s observations.

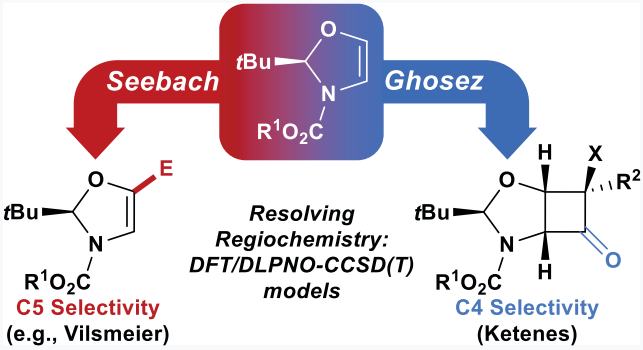

INTRODUCTION

In 1905 1907, long before the discovery of the Diels Alder reaction, Hermann Staudinger reported the isolation of diphenylketene and its unique ability to form a four-membered ring by addition to cyclopentadiene.[1] At the time, this pioneering work remained of little synthetic value due to the rapid dimerization of most alkyl and aryl ketenes that favorably competed with the desired alkene cycloaddition. It took about 50 years to witness a real renaissance of ketene cycloaddition chemistry, with ketenes rendered synthetically useful by observations of their facile cycloadditions with newly available activated olefins such as enamines,[2] and the development of highly electrophilic haloketenes that enabled stereospecific cycloadditions to a wide variety of olefins.[3] In the ensuing decades, this reaction has become undoubtedly one of the most important methods for the generation of four-membered rings.[4]

During the renaissance era of ketene chemistry, Woodward and Ho mann emphasized the role of the π orbital of the ketene C O bond as the "spearhead" of its reactivity.[5] They described these reactions as $[_{\pi}2_s + _{\pi}2_a]$ cycloadditions, driven by the perpendicular interaction of the alkene π orbital with the ketene C O π orbital. Early computational studies showed that thermal (2 + 2) cycloadditions of ketenes and alkenes proceeded via either a stepwise or concerted, asynchronous mechanism.[6] In 1990, Wang and Houk performed theoretical investigations on the reaction of ketenes with alkenes utilizing the *ab initio* SCF method with STO-3G, 3-21G, and 6-31G basis sets and correlation energy corrections at the MP2 level.[7] These studies concluded that the reactions are (2 + 2 + 2) cycloadditions, another way that ketene cycloadditions had been analyzed by Woodward and Ho mann.[5] Yamabe et al. further investigated the frontier molecular orbital (FMO) interactions involved in ketene (2 + 2) cycloadditions using *ab initio* methods.[8] These results demonstrated that the (2 + 2) cycloadditions proceed via a concerted, asynchronous mechanism involving two independent FMO interactions: the first FMO interaction involves an overlap of a π orbital or a nonbonding orbital of the ketenophile with the LUMO of the ketene, while the second interaction implicates overlap of the π orbital of the ketenophile with the HOMO of the ketene.[8] By 2006, Singleton utilized density functional theory (DFT) to study the reaction of cyclopentadiene with diphenylketene and dichloroketene using the ωB97X-D and mPW1K functionals.[6c] Singleton s results demonstrated that the carbonyl group of the ketene can participate in both (4 + 2) and (2 + 2) cycloadditions. More recently, Tang and co-workers studied the mechanism of Lewis acid-promoted (2 + 2) cycloadditions of ketenes and alkenes DFT.[9] Despite the progress made

Received: January 1, 2022
Published: January 25, 2022

https://doi.org/10.1021/acs.joc.2c00001
J Org Chem 2022 87 3613 3622

Scheme 1. Divergent Regioselectivities in the Reaction of)-2-*tert*-Butyldihydrooxazoles with Ketenes and Acylating Agents[10,12]

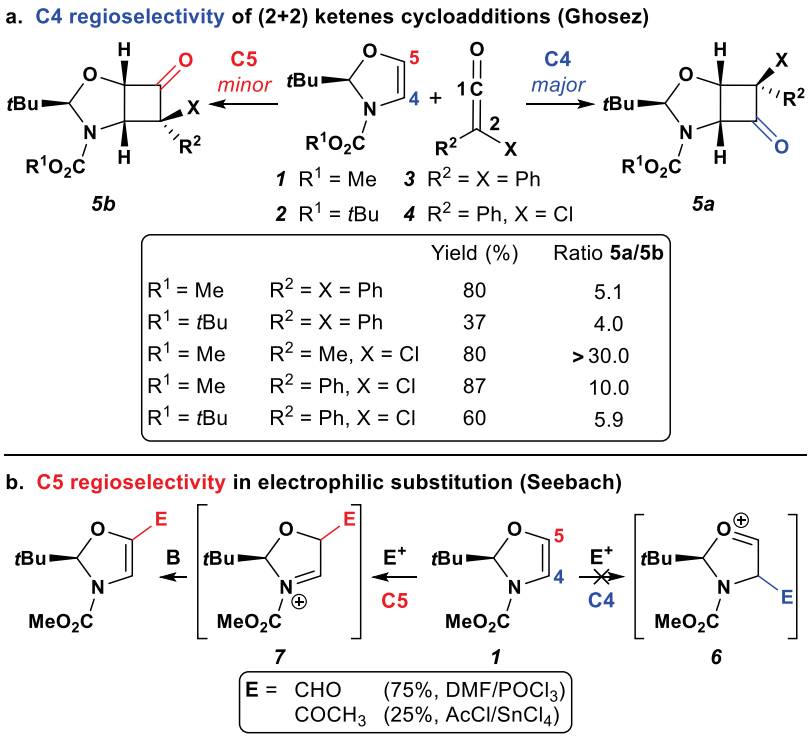

Figure 1. Relative energies of the iminium and oxonium ions of oxazolines **1** and **2**. Energies are provided in units of kcal/mol at the ωB97X-D/6-311++G(d,p) level.

toward understanding the reactivity of ketenes using computations, no theoretical studies have been performed to elucidate substituent e ects on regioselectivity in the thermal (2 + 2) cycloadditions of ketenes with nonsymmetric alkenes such as dihydrooxazoles (oxazolines) studied by Ghosez et al.

The regioselectivity of these ketene-plus-alkene cycloadditions was expected to be that observed for the addition of electrophilic reagents to alkenes, i.e., the electrophilic central atom of the ketene should bind to the more nucleophilic carbon atom of olefin.[4] We were therefore intrigued by the unprecedented regioselectivity trend observed in Ghosez s work on ketene/oxazoline (2 + 2) cycloadditions.[10] Ghosez and co-workers observed that a variety of ketenes reacted with oxazolines **1** and **2** to give preferentially (2 + 2) cycloadducts **5a**, resulting from an attack of C4 of oxazolines **1** and **2** on the electrophilic C O of the ketene (30 79 yields, Scheme 1a) with only minor yields of the previously "expected" regioisomers **5b**.[11] These oxazolines had been shown by Seebach et al. to be versatile synthons containing a highly reactive electron-rich C C bond amenable to significant elaboration.[12] Acylating reagents utilized in Seebach s studies (Vilsmeier reagent and acetyl chloride) were added at the C5 position selectively on the face opposite to the *tert*-butyl substituent. This regioselectivity has been explained on the basis of the preferential formation of acyliminium ion intermediate **7**, which is more stable than the oxonium ion **6** resulting from an attack at C4.[13]

Seeking to rationalize this disparity in regioselectivity, we undertook a computational study of the thermal (2 + 2) cycloadditions between (*R*)-2-*tert*-butyldihydrooxazoles and diphenyl- and phenylchloroketenes.

RESULTS AND DISCUSSION

We began our investigation with Seebach s proposal that regiochemistry of electrophilic addition to oxazolines is dictated by the stability of the resulting heteroatom-stabilized carbocation.[13] The oxonium and iminium ions of oxazolines **1** and **2** are shown in Figure 1. Relative to iminium ions **8** and **10**, the oxonium ions **9** and **11** are destabilized by several kcal/mol, even though the iminium ions are substituted by electron-withdrawing esters. This is consistent with Seebach s proposal and earlier calculations: the greater stability of intermediates **8** and **10** suggests the preferential attack of electrophiles at C5 of oxazolines.

However, these data are inconsistent with Ghosez s regiochemical observations, and we continued to a complete

https://doi.org/10.1021/acs.joc.2c00001
J Org Chem 2022 87 3613 3622

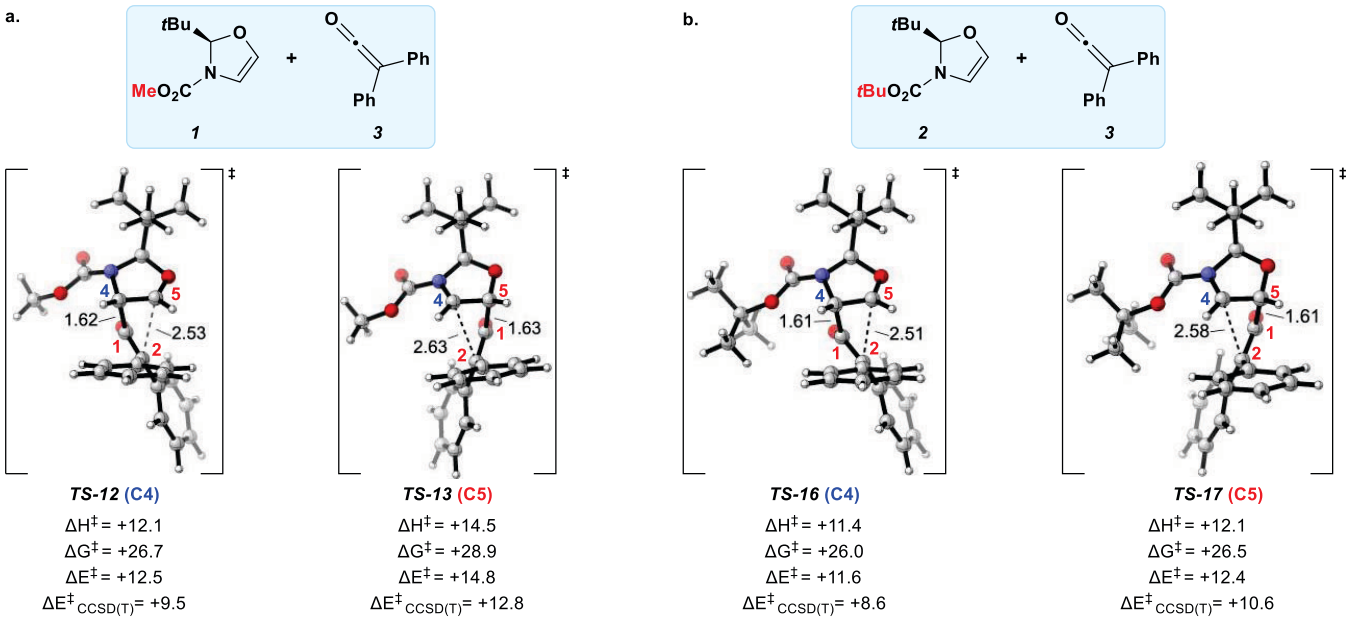

Figure 2. Regioisomeric transition-state structures and calculated energies for the (2 + 2) cycloadditions of diphenylketene **3** with oxazolines (a) **1** and (b) **2**. Geometry optimization was conducted at the ωB97X-D/6-311++G(d,p) level of theory. Single-point energies were calculated with ωB97X-D/6-311++G(2d,2p) and DLPNO-CCSD(T)/cc-pVTZ. Energies are provided in units of kcal/mol.

Scheme 2. Energy Pro le for the Reaction of Carbomethoxy-Substituted Oxazoline 1 and Ketene 3[a]

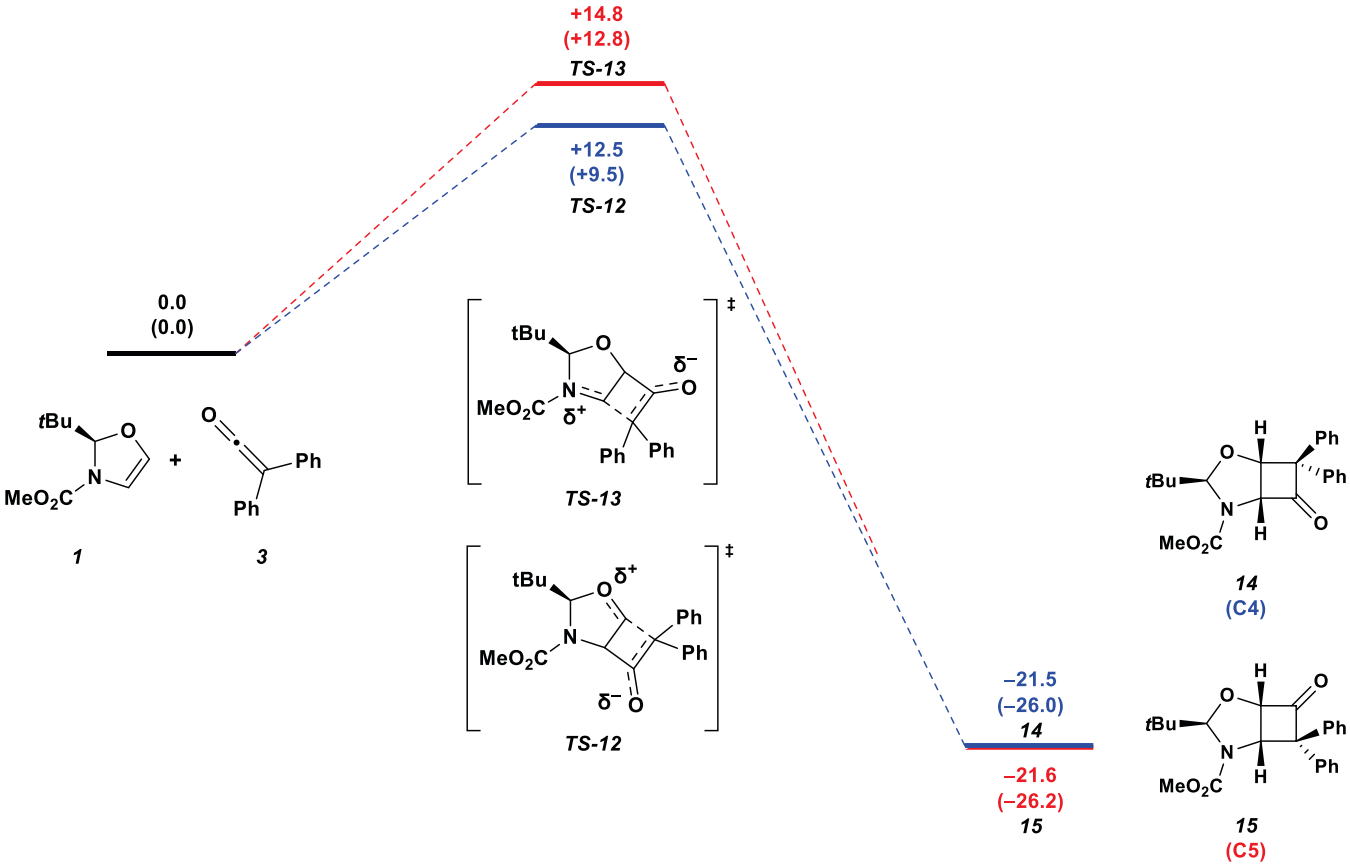

[a]Geometry optimization was conducted at the ωB97X-D/6-311++G(d,p) level of theory. Single-point energies were calculated with both ωB97X-D/6-311++G(2d,2p) (shown in plain text) and DLPNO-CCSD(T)/cc-pVTZ (shown in parentheses). Energies are provided in units of kcal/mol.

examination of the potential energy surface of ketene (2 + 2) cycloaddition with oxazolines. Figure 2 shows transition-state structures for the (2 + 2) cycloaddition of oxazolines **1** and **2** with diphenylketene **3**. The carbomethoxy-substituted oxazoline **1** gives rise to transition states **TS-12** and **TS-13**, proceeding from initial electrophilic addition to C4 and C5,

https://doi.org/10.1021/acs.joc.2c00001
J Org Chem 2022 87 3613 3622

Scheme 3. Energy Pro le for the Reaction of *tert*-Butoxycarbonyl-Containing Oxazoline 2 and Ketene 3[a]

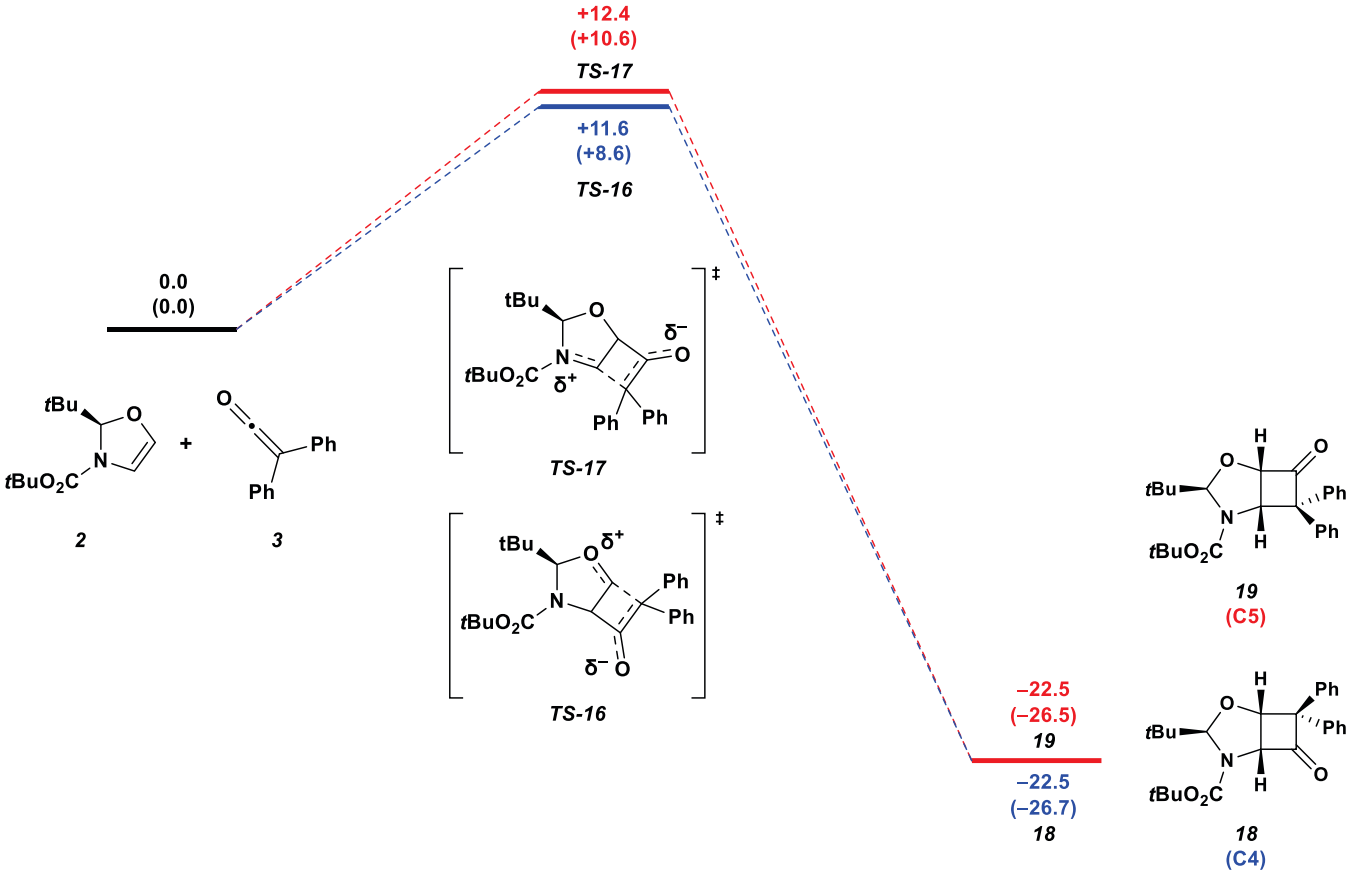

[a]Geometry optimization was conducted at the ωB97X-D/6-311++G(d,p) level of theory. Single-point energies were calculated with both ωB97X-D/6-311++G(2d,2p) (shown in plain text) and DLPNO-CCSD(T)/cc-pVTZ (shown in parentheses). Energies are provided in units of kcal/mol.

respectively. Oxazoline **2**, carrying a *tert*-butoxycarbonyl group, similarly proceeds to transition states **TS-16** and **TS-17**. Structures **TS-12** and **TS-16**, leading to cycloadducts containing a carbonyl group α to the oxazoline nitrogen atom, were calculated to be more stable than their regioisomeric counterparts. Our investigation additionally found that the (2 + 2) cycloaddition advances through a highly asynchronous, concerted mechanism, where the length of the first formed bond varies substantially. Single-point energies calculated with ωB97X-D/6-311++G(2d,2p) generally agree with those obtained with DLPNO-CCSD(T)/cc-pVTZ. These data are consistent with the preferential formation of the initial oxazoline ketene bond at C4, as observed by Ghosez (Scheme 1).

The energy profiles for the cycloaddition of oxazolines **1** and **2** with diphenylketene **3** are shown in Schemes 2 and 3, respectively. Cycloadditions occurring via **TS-12** and **TS-16** are shown to be kinetically favored, and despite little to no energy di erence between diastereomeric products, they yield the C4-(α-keto) adducts **14** and **18**, respectively. In these diagrams, we show the highest energy point along the reaction coordinate as the transition state of the reaction.

We proceeded to examine the (2 + 2) cycloaddition of oxazoline **1** with the asymmetrically substituted phenylchloroketene **4**. Due to the asymmetry, the cycloaddition can proceed with either chloro-*endo* or phenyl-*endo* diastereoselectivity; the corresponding transition states (**TS-20** **TS-23**) are shown in Figure 3a. Similar to the cycloaddition of **1** and **3**, the major transition states involve an attack of the central carbon of the ketene on C4 of the oxazoline, to the oxygen atom. This cycloaddition has a 7 kcal/mol lower barrier than that of diphenylketene, as expected due to the inductive electron withdrawal and smaller steric e ect of the Cl. Single-point energy calculations at the ωB97X-D/6-311++G(2d,2p) and DLPNO-CCSD(T)/cc-pVTZ levels confirmed that these reactions also proceeded via a highly asynchronous mechanism. Careful optimization yielded an extremely shallow intermediate along the reaction coordinate, representing an energy plateau on the ascent to transition states homologous to those of the diphenylketene case (see the SI). We hypothesize that this structure is indicative of a highly asynchronous cycloaddition for phenylchloroketene, as the free-energy di erence between the initial bond-forming transition structure and the intermediate is essentially zero.

Calculations at the ωB97X-D/6-311++G(2d,2p) level of theory suggest no di erence in activation energy between Ph-*endo* and Cl-*endo* transition structures, though single-point energy corrections at the higher DLPNO-CCSD(T)/cc-pVTZ theory level demonstrate a strong preference for the Ph-*endo* TS in accord with experimental observations (**TS-20**, $E_{CCSD(T)}$ = 2.6 kcal/mol relative to Cl-*endo* transition state **TS-21**). While the corresponding Ph-*endo* product is more crowded than the Cl-*endo*, the product is favored because it actually has a sterically less congested transition state where the phenyl substituent is oriented away from the alkene (Figure 3).

https://doi.org/10.1021/acs.joc.2c00001
J Org Chem 2022 87 3613 3622

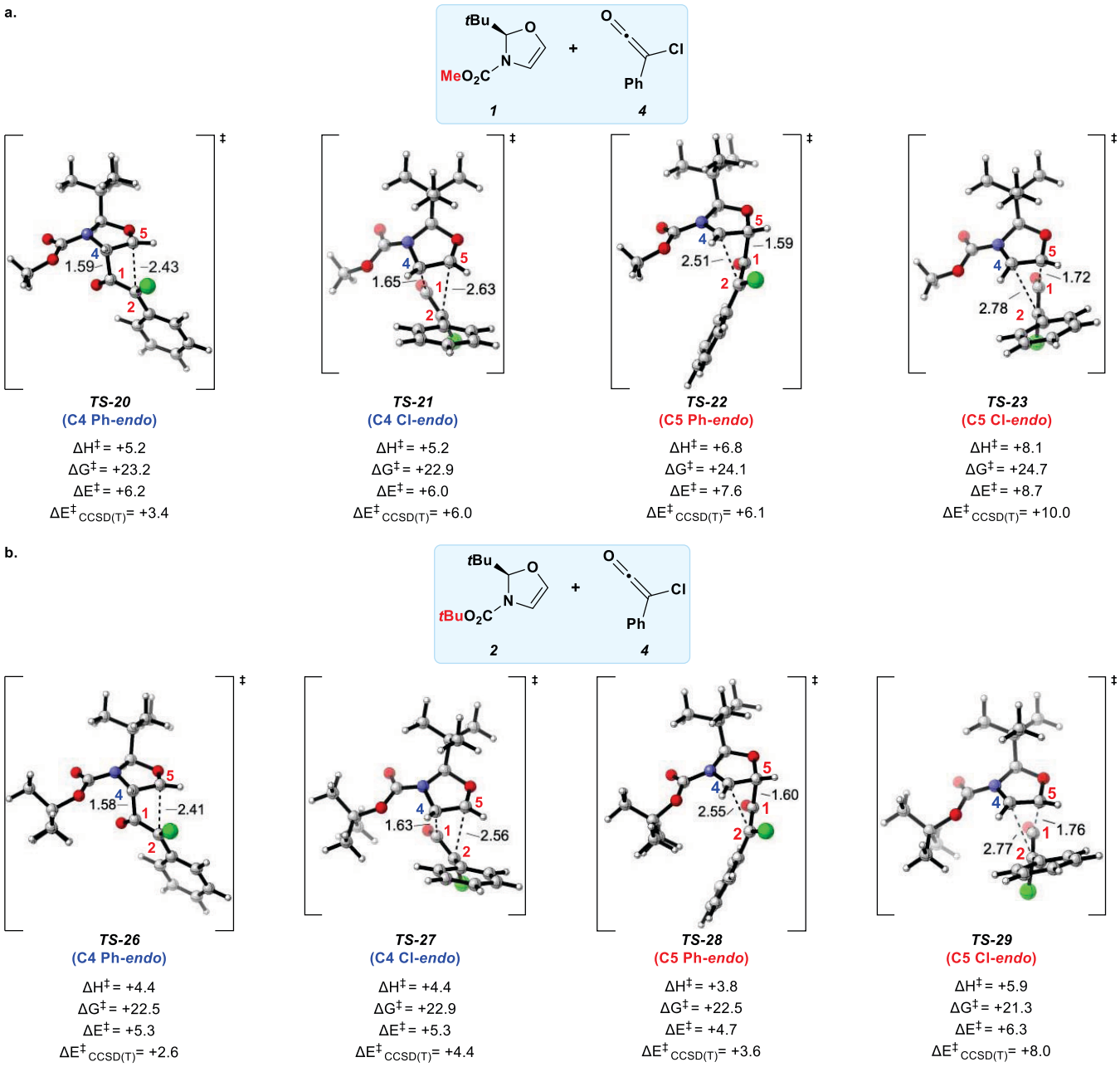

Figure 3. Regioisomeric transition structures and calculated energies for the (2 + 2) cycloadditions of phenylchloroketene **4** with oxazolines (a) **1** and (b) **2**, respectively. Geometry optimization was conducted at the ωB97X-D/6-311++G(d,p) level of theory. Single-point energies were calculated with ωB97X-D/6-311++G(2d,2p) and DLPNO-CCSD(T)/cc-pVTZ. Energies are provided in units of kcal/mol.

For the regioisomeric addition of the electrophilic carbon to the oxazoline C5 (to the nitrogen), DLPNO-CCSD(T)/cc-pVTZ single-point energies again suggest that the reaction occurs selectively via the Ph-*endo* transition state **TS-22** ($E_{CCSD(T)}$ = 3.9 kcal/mol relative to Cl-*endo*). Between the favored Ph-*endo* cycloadditions, the activation energy of the major reaction at the C4 position (**TS-20**) is several kcal/mol lower than that of the minor reaction at the C5 position ($E_{CCSD(T)}$ = 2.7 kcal/mol, $E_{\omega B97X\text{-}D}$ = 1.4 kcal/mol, Scheme 4).

We also investigated the (2 + 2) cycloaddition of *tert*-butyloxycarbonyl-substituted oxazoline **2** with phenylchloroketene **4** (Figure 3b, Scheme 5). According to the experimental investigation by the Ghosez group, the reactions with the oxazoline containing a *tert*-butyloxycarbonyl protecting group are less regioselective and lower yielding than the methylated analogue. Figure 3b shows that transition states **TS-26** (Ph-*endo*) and **TS-27** (Cl-*endo*) involve the addition of the central carbon of ketene **4** onto C4 of oxazoline **2**. DLPNO-CCSD(T)/cc-pVTZ single-point energies suggest that the reaction occurs selectively via the Ph-*endo* transition state **TS-26** ($E_{CCSD(T)}$ = 1.8 kcal/mol vs Cl-*endo*).

The regioisomeric attack onto C5 of the oxazoline occurs similarly via transition states with Cl-*endo* or Ph-*endo* (**TS-28**, **TS-29**, respectively; Figure 3). DLPNO-CCSD(T)/cc-pVTZ single-point energies again suggest that cycloaddition favors the Ph-*endo* transition state **TS-28** ($E_{CCSD(T)}$ = 4.4 kcal/mol relative to Cl-*endo*).

For Ph-*endo* cycloadditions, DLPNO-CCSD(T)/cc-pVTZ single-point energy of the major reaction at the C4 position

https://doi.org/10.1021/acs.joc.2c00001
J Org Chem 2022 87 3613 3622

Scheme 4. Energy Pro le for the Reaction of Carbomethoxy-Containing Oxazoline 1 and Chlorophenylketene 4 Leading to Regioisomeric Ph-*endo* Adducts 24 and 25[a]

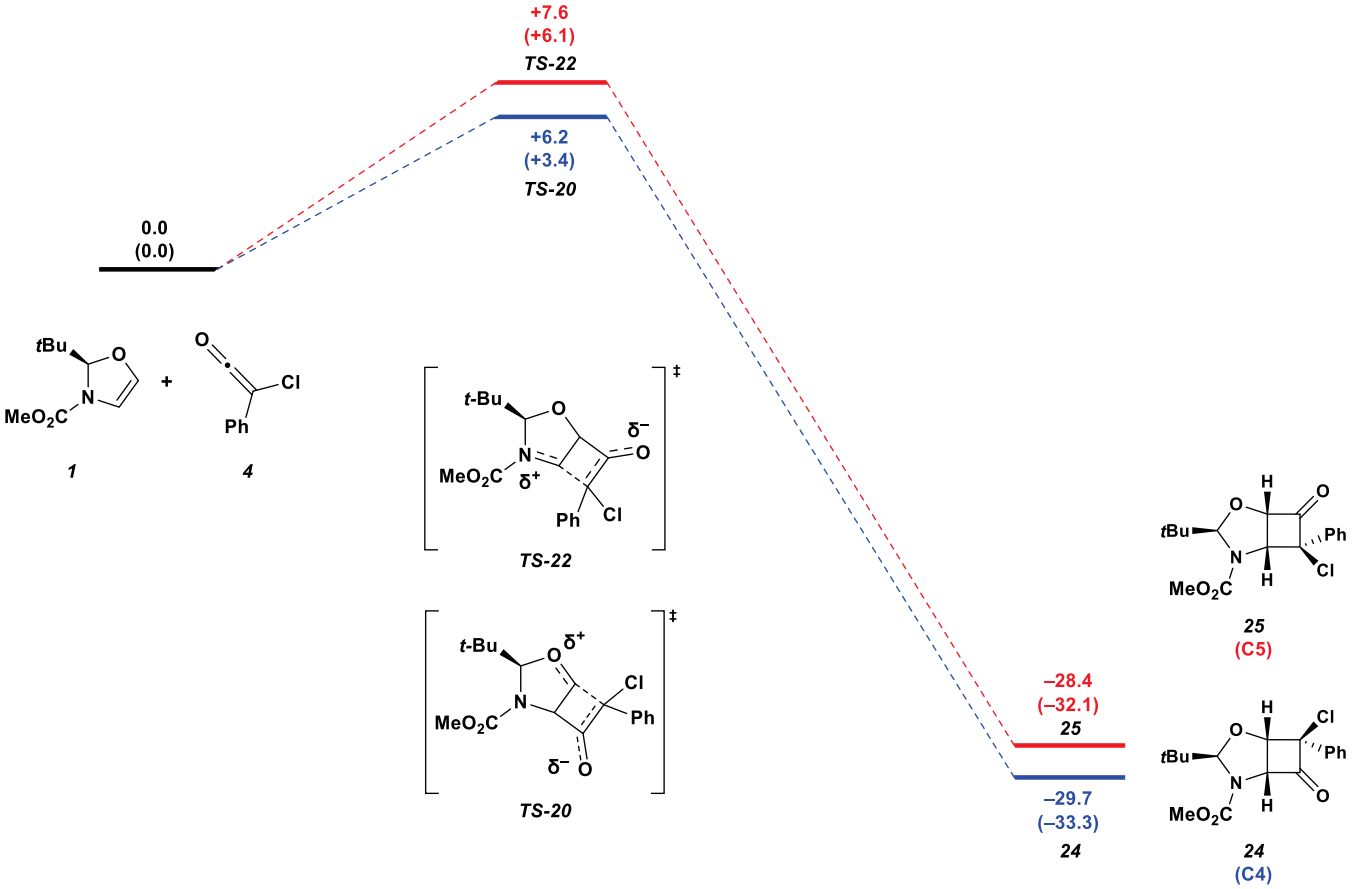

[a]Geometry optimization was conducted at the ωB97X-D/6-311++G(d,p) level of theory. Single-point energies were calculated with ωB97X-D/6-311++G(2d,2p) (shown in plain text) and DLPNO-CCSD(T)/cc-pVTZ (shown in parentheses). Energies are in units of kcal/mol.

(**TS-26**) is 1.0 kcal/mol lower than that of the minor reaction at the C5 position (**TS-28**). However, ωB97X-D/6-311++G(2d,2p) single-point energies suggest that cycloaddition favors the formation of **TS-28** reaction by 0.6 kcal/mol. Both methods predict lower selectivity as found experimentally for the *tert*-butyl compound, although the ωB97X-D/6-311++G(2d,2p) results predict the wrong major regioisomer. Gratifyingly, the higher level of theory predicts the regioisomer consistent with experimental observation.

Intriguingly, our calculations on Ghosez s ketene cycloadditions to oxazolines all support the addition of the ketene electrophilic carbon to the oxazoline C4 in contradiction to Seebach s acylation results. To further investigate the electronic profile of these cycloadditions, we performed a natural population analysis (NPA). The FMOs of oxazolines **1** and **2** and ketenes **3** and **4** were obtained and are shown in Figure 4. The thermal (2 + 2) cycloadditions of ketenes and alkenes should involve the interaction of the π orbital of the alkene C C bond (i.e., the oxazoline HOMO) and the π orbital of the ketene C O bond (i.e., the ketene LUMO). The π orbitals of oxazolines **1** and **2** have larger MO coefficients at C4: for oxazoline **1**, the HOMO coefficients in the NAO basis of C4 and C5 are 0.28 and 0.25, respectively, and for oxazoline **2**, the HOMO coefficients of C4 and C5 are 0.27 and 0.25, respectively. Similarly, the π orbitals of ketenes **3** and **4** exhibit larger MO coefficients on the central carbon. While the di erence in C4/C5 HOMO coefficients is small in both oxazolines, the larger coefficients suggest that reactivity at C4 should be favored as observed.

We also investigated the natural bond order (NBO) charges of oxazolines **1** and **2** to better understand the origins of regioselectivity (Table 1). For the reactants, the NBO charges of oxazoline **1** at C4 and C5 are 0.10 and 0.13, respectively. Similarly, the NBO charges of oxazoline **2** at C4 and C5 are 0.10 and 0.12, respectively. Unlike the oxazoline orbital coefficients, here there are rather dramatic di erences; the charges predict that C4 is more nucleophilic (more negative) than C5, again consistent with Ghosez s results. This is likely an inductive e ect rising from the ethereal oxygen withdrawing electron density from C5.

Therefore, C C bond formation between C1 of ketene **3** or **4** and C4 of oxazolines occurs more readily than that between C1 of the ketenes and C5 of oxazolines. At the transition state, the NBO charge of the C4 of the minor pathway is 0.19 or 0.20, while that of the C5 carbon atom of major pathway is 0.36 or 0.37. Thus, the computational results demonstrate that the HOMO coefficients and NBO charges of oxazolines **1** and **2** correlate with experimental regioselectivities in the (2 + 2) cycloaddition with ketenes **3** and **4**.

Our calculations of the full ketene/oxazoline (2 + 2) cycloaddition, NPA, and NBO analyses all suggest that electrophilic addition to C4 should be favored. Indeed, viewing ketene as an acylating agent alone, there is little immediate di erence between the substrate the Vilsmeier and Friedel

https://doi.org/10.1021/acs.joc.2c00001
J Org Chem 2022 87 3613 3622

Scheme 5. Energy Pro le for the Reaction of *tert*-Butoxycarbonyl-Containing Oxazoline 2 and Chlorophenylketene 4 Leading to Regioisomeric Ph-*endo* Adducts 30 and 31[a]

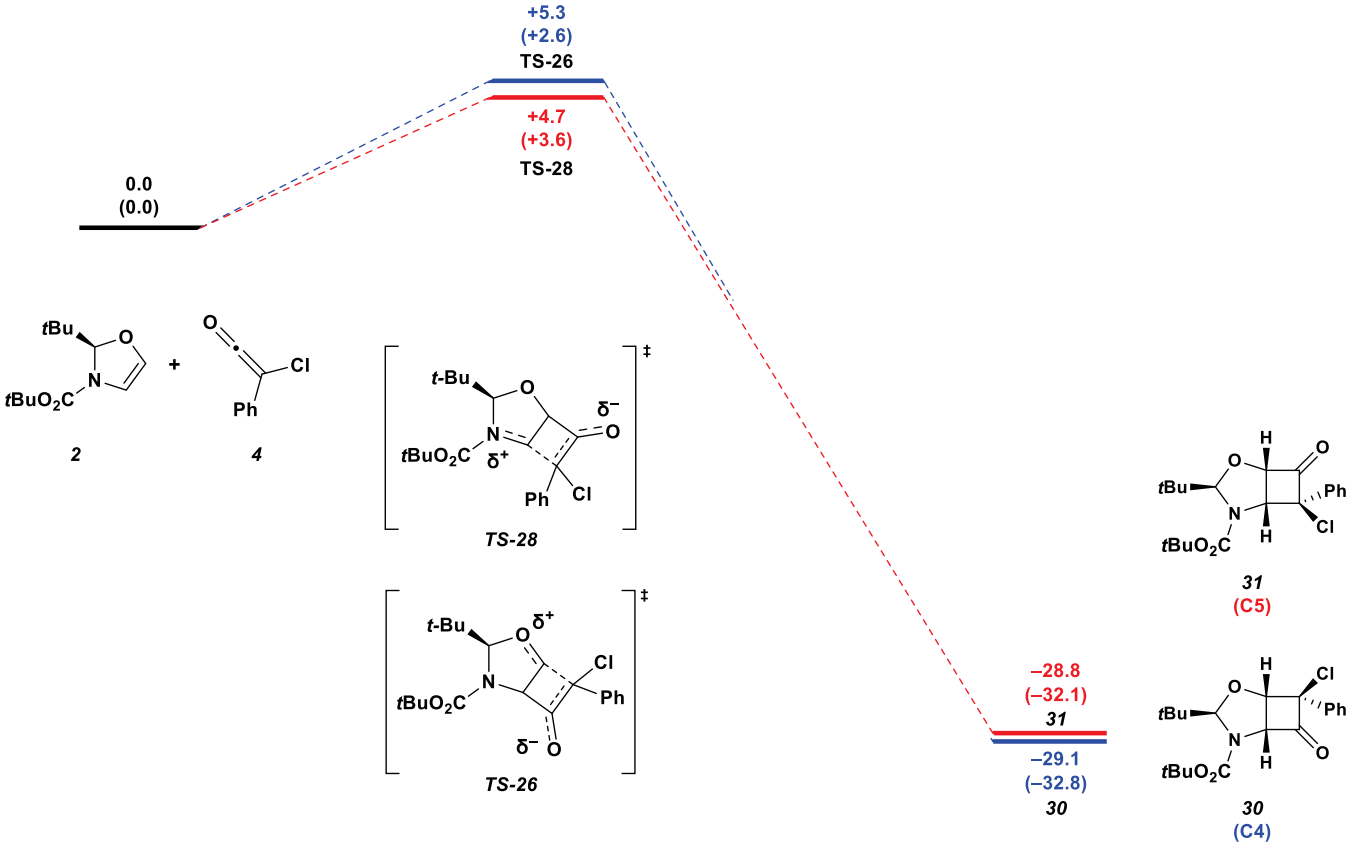

[a]Geometry optimization was conducted at the ωB97X-D/6-311++G(d,p) level of theory. Single-point energies were calculated with ωB97X-D/6-311++G(2d,2p) (shown in plain text) and DLPNO-CCSD(T)/cc-pVTZ (shown in parentheses). Energies are in units of kcal/mol.

Crafts reagents employed by Seebach for oxazoline acylation. Yet, the Vilsmeier and Friedel Crafts starting reagents are cationic species, while the ketenes studied by Ghosez are neutral. These charges may influence the buildup of charge in the transition structure and have direct implications for Seebach s stabilization model (Figure 1) relative to the ketene additions studied here.

Seeking comparison between these reagents—and therefore the disparate regiochemical outcome—we expanded our study to include the transition structures of the Vilsmeier reagent cation with oxazoline **1** (Figure 5). In accordance with Seebach s results, the C5 addition TS is found to be more stable than the corresponding C4 addition ($E_{CCSD(T)}$ = 2.3 kcal/mol vs C4). An NBO charge analysis of the two transition structures, **TS-V-C4** and **TS-V-C5**, demonstrates the influence of the starting material charge on the selectivity (Table 1). In comparison to the ketene + oxazoline system (e.g., **1** + **3**), Vilsmeier reagent addition to C4 builds up more positive charge density on C4 and the oxazoline oxygen than the corresponding ketene addition. This is consistent with the polarizing e ect of a cationic electrophile on the donor oxygen: as oxygen is a poorer electron donor than nitrogen (Figure 1), the buildup of positive charge in transition structure **TS-V-C4** reflects an increased energy barrier. Therefore, cationic acylating agents such as the Vilsmeier reagent are expected to react primarily at C5, as demonstrated by Seebach.

In contrast, the ketenes do not induce as much positive charge due to their highly asynchronous, concerted interactions with the oxazoline π-system. The four-membered character of the transition structure precludes the formation of a true, heteroatom-stabilized carbocation. Therefore, regioselectivity reflects the most nucleophilic center, which as shown is C4, as observed by Ghosez.

CONCLUSIONS

These DFT calculations elucidate the concerted, highly asynchronous, mechanism for the thermal (2 + 2) cycloadditions of oxazolines **1** and **2** with diphenyl- and dichloroketenes **3** and **4**. The cycloadditions involve regioselective addition of the central carbon of the ketene π-system onto C4 of oxazolines, which is consistent with experimental results obtained by the Ghosez group. In addition, we explore Cl-*endo* and Ph-*endo* stereoselectivities in the (2 + 2) cycloadditions of oxazolines with phenylchloroketene. The DLPNO-CCSD(T)/cc-pVTZ single-point energies suggest that cycloaddition favors the Ph-*endo* reaction in agreement with the experimental results.

These results, together with a study of Seebach s addition of the Vilsmeier reagent to oxazolines, elucidate the origins of acylating agent regioselectivity with oxazolines. Due to the buildup of charge in the oxazoline, charged electrophiles are expected to react at C5, to the nitrogen, to produce the more stabilized acyl-amino cation system, as predicted by Seebach. The corresponding ketene addition is expected to proceed at the more nucleophilic C4, to the oxygen, as the

https://doi.org/10.1021/acs.joc.2c00001
J Org Chem 2022 87 3613 3622

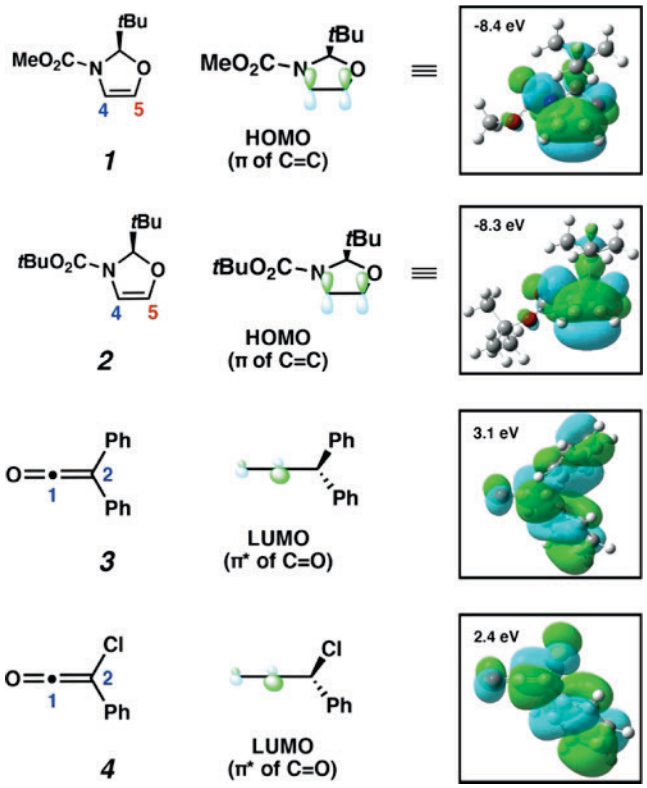

Figure 4. FMOs of oxazolines **1** and **2** and ketenes **3** and **4**. FMOs were generated at the HF/6-31G(d)//ωB97X-D/6-311++G(d,p) level.

Table 1. NBO Charges of the Reactants and Transition States for the 2 + 2) Cycloadditions of Oxazolines 1 and 2 with Ketenes and Oxazoline 1 with Vilsmeier Reagent at the B97X-D/6-311++G 2d,2p) Level[a]

	ketenes	C4	C5	N	O	R
1		0.10	0.13	0.56	0.57	0.35
2		0.10	0.12	0.55	0.57	0.39
3	0.00					
4	0.00					
TS-12	0.41	0.15	0.37	0.57	0.49	0.36
TS-13	0.45	0.19	0.04	0.51	0.58	0.37
TS-16	0.41	0.14	0.37	0.57	0.49	0.40
TS-17	0.45	0.20	0.04	0.51	0.58	0.42
TS-20	0.40	0.14	0.36	0.58	0.50	0.36
TS-22	0.44	0.19	0.04	0.52	0.58	0.37
TS-26	0.37	0.16	0.36	0.58	0.50	0.40
TS-28	0.49	0.20	0.04	0.51	0.58	0.43
TS-V-C4		0.11	0.38	0.58	0.46	
TS-V-C5		0.13	0.08	0.51	0.58	

[a]R = remaining atoms on ketenophile.

asynchronous, concerted mechanism reduces charge buildup, preventing the formation of a full carbocation.

COMPUTATIONAL METHODS

Quantum mechanical calculations were performed with Gaussian 16.[14] Geometry optimization was completed using the mPW1PW91[15] and ωB97X-D[16] functionals with the 6-311++G(d,p) basis set. Reactions of oxazolines with diphenylketene and phenylchloroketene were studied both in the gas phase and using the SMD solvation model[17] for toluene at 298 K and cyclohexane at 333 K. Frequency

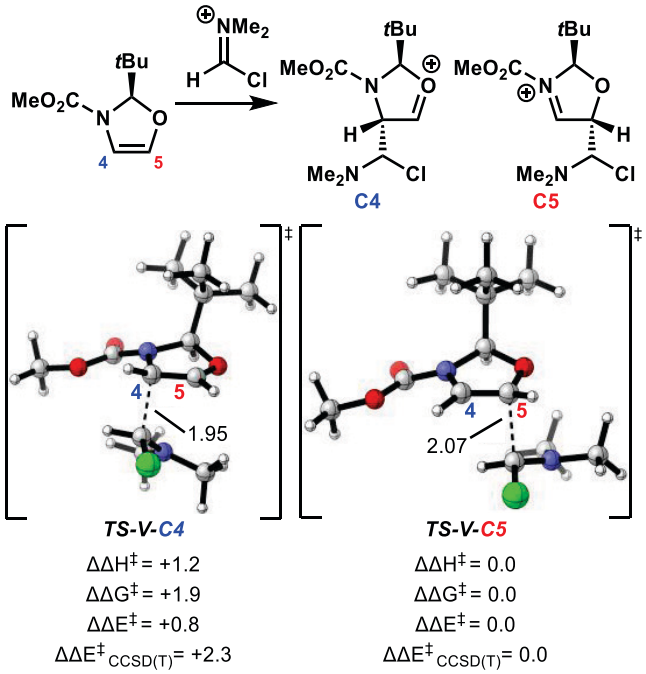

Figure 5. Regioisomeric transition structures and calculated energies for the addition of Vilmeier reagent cation to oxazoline **1**. Geometry optimization was conducted at the ωB97X-D/6-311++G(d,p) level of theory. Single-point energies were calculated with ωB97X-D/6-311++G(2d,2p) and DLPNO-CCSD(T)/cc-pVTZ. Energies are provided in units of kcal/mol relative to the energies of **TS-V-C5**.

calculations were performed at the same theoretical level as that used for geometry optimizations to verify the stationary points as either minima or first-order saddle points on the potential energy surface. Intrinsic reaction coordinate (IRC) calculations were performed to confirm that saddle points corresponded to the desired transition states. A quasiharmonic Grimme correction with a frequency cuto value of 100 cm ^{1} was applied for ions **8** **11** using Paton s Goodvibes software.[18] DLPNO-CCSD(T)[19] single-point energy calculations were performed with a cc-pVTZ[20] basis set and the SMD solvation model on ORCA 4.0.1.[21] Additional single-point calculations were carried out at the ωB97X-D/6-311++G(2d,2p) level. Natural atomic orbitals (NAO) were calculated using Multiwfn.[22] Detailed energies, enthalpies, and free energies of stationary points, as well as the results from mPW1PW91 calculations, are provided in the Supporting Information. Molecular structures were illustrated using CYLview.[23]

ASSOCIATED CONTENT

Supporting Information

The Supporting Information is available free of charge at https://pubs.acs.org/doi/10.1021/acs.joc.2c00001.

Computational analysis of the addition reaction with phenylchloroketene 4, tabulated energies, and Cartesian coordinates of all optimized structures (PDF)

AUTHOR INFORMATION

Corresponding Authors

Léon Ghosez *Laboratoire ORSY UCLouvain 1348 Louvain-la-Neuve Belgium;* Present Address: European Institute of Chemistry and Biology (IECB), University of Bordeaux, CNRS, CBMN 5248, Bordeaux INP, 2 Rue Robert Escarpit, FR-33607 Pessac, France; Email: l.ghosez@iecb.u-bordeaux.fr

K N Houk *Department of Chemistry and Biochemistry University of California Los Angeles California 90095*

https://doi.org/10.1021/acs.joc.2c00001
J Org Chem 2022 87 3613 3622

United States; orcid.org/0000-0002-8387-5261; Email: houk@chem.ucla.edu

Authors

Ledong Zhu *Department of Chemistry and Biochemistry University of California Los Angeles California 90095 United States*

Mark A Maskeri *Department of Chemistry and Biochemistry University of California Los Angeles California 90095 United States;* orcid.org/0000-0002-2630-8930

Melissa Ramirez *Department of Chemistry and Biochemistry University of California Los Angeles California 90095 United States;* orcid.org/0000-0002-4038-2029

F Le Bideau *Laboratoire ORSY UCLouvain 1348 Louvain-la-Neuve Belgium;* Present Address: Université de Paris-Saclay, CNRS, BioCIS, 92290 Châtenay-Malabry, France

Complete contact information is available at: https://pubs.acs.org/10.1021/acs.joc.2c00001

Notes

The authors declare no competing financial interest.

ACKNOWLEDGMENTS

The authors are grateful to the National Science Foundation for financial support of this research (CHE-1764328). Computations were performed on the Ho man2 cluster at UCLA and the Expanse cluster available from the NSF XSEDE program under grant OCI-1053575. The authors belatedly dedicate this manuscript to the memory of our dear friend and fantastic scientist Bernd Giese, on the occasion of his 80th birthday.

REFERENCES

(1) (a) Staudinger, H. Ketene, eine neue Körperklasse. *Ber. Dtsch. Chem. Ges.* **1905**, *38*, 1735 1739. (b) Staudinger, H. Über ketene. 4. Mitteilung: Reaktionen des diphenylketens. *Ber. Dtsch. Chem. Ges.* **1907**, *40*, 1145 1148.

(2) (a) Hasek, R.; Martin, J. Communications-Cycloaddition of Ketenes to Enamines. *J. Org. Chem.* **1961**, *26*, 4775 4776. (b) Berchtold, G.; Harvey, G.; Wilson, J.G. Communications-The Reaction of Enamines with Ketene. *J. Org. Chem.* **1961**, *26*, 4776. (c) Opitz, G.; Kleemann, M.; Zimmermann, F. Abfangen von Ketenen durch Cycloaddition an Enamine. *Angew. Chem.* **1962**, *74*, 32.

(3) (a) Stevens, H. C.; Reich, D. A.; Brandt, D. R.; Fountain, K. R.; Gaughan, E. J. A New Tropolone Synthesis via Dichloroketene. *J. Am. Chem. Soc.* **1965**, *87*, 5257 5259. (b) Ghosez, L.; Montaigne, R.; Mollet, P. Cycloadditions with dichloroketene. *Tetrahedron Lett.* **1966**, *7*, 135 139. (c) Montaigne, R.; Ghosez, L. Stereospecific cis Addition of Dichloroketene to cis-and trans-Cyclooctenes. *Angew. Chem. Int. Ed.* **1968**, *7*, 221. (d) Ghosez, L.; Montaigne, R.; Roussel, A.; Vanlierde, H.; Mollet, P. Cycloadditions of dichloroketene to olefins and dienes. *Tetrahedron* **1971**, *27*, 615 633.

(4) (a) Fu, N.; Tidwell, T. T. Cycloaddition and electrocyclic reactions of vinylketenes, allenylketenes, and alkynylketenes. *Org. React.* **2015**, *87*, 257 506. (b) Heravi, M. M.; Talaei, B. Ketenes as Privileged Synthons in the Syntheses of Heterocyclic Compounds. Part 1: Three- and Four-Membered Heterocycles. In *Advances in Heterocyclic Chemistry*; Elsevier, 2014; Vol. *113*, pp 143 244. (c) Alcaide, B.; Aragoncillo, C.; Almendros, P. 5.02 Thermal Cyclobutane Ring Formation. In *Comprehensive Organic Synthesis*; Elsevier, 2014; Vol. *5*, pp 66 84. (d) Nelson, S. G.; Dura, R. D.; Peelen, T. J. Catalytic Asymmetric Ketene [2+ 2] and [4+ 2] Cycloadditions. *Org. React.* **2012**, *82*, 471 621. (e) Pellissier, H. Formation of 3-, 4-and 5-Membered Cycles by Intermolecular Reactions. In *Comprehensive Enantioselective Organocatalysis: Catalysts Reactions and Applications*; Wiley-VCH, 2013; pp 1091 1130. (f) Allen, A. D.; Tidwell, T. T. Ketenes and other cumulenes as reactive intermediates. *Chem. Rev.* **2013**, *113*, 7287 7342.

(5) Woodward, R. B.; Hoffmann, R. The conservation of orbital symmetry. *Angew. Chem. Int. Ed.* **1969**, *8*, 781 853.

(6) (a) Allen, A. D.; Tidwell, T. T. Structure and Mechanism in Ketene Chemistry. In *Advances in Physical Organic Chemistry*; Elsevier, 2014; Vol. *48*, pp 229 324. (b) Machiguchi, T.; Hasegawa, T.; Ishiwata, A.; Terashima, S.; Yamabe, S.; Minato, T. Ketene Recognizes 1, 3-Dienes in Their s-Cis Forms through [4+ 2](Diels Alder) and [2+ 2](Staudinger) Reactions. An Innovation of Ketene Chemistry. *J. Am. Chem. Soc.* **1999**, *121*, 4771 4786. (c) Ussing, B. R.; Hang, C.; Singleton, D. A. Dynamic effects on the periselectivity, rate, isotope effects, and mechanism of cycloadditions of ketenes with cyclopentadiene. *J. Am. Chem. Soc.* **2006**, *128*, 7594 7607.

(7) Wang, X.; Houk, K. N. Carbenoid character in transition structures for reactions of ketenes with alkenes. *J. Am. Chem. Soc.* **1990**, *112*, 1754 1756.

(8) (a) Yamabe, S.; Minato, T.; Osamura, Y. Dual one-centre frontier-orbital interactions in [2+ 2] cycloadditions of ketenes. *J. Chem. Soc. Chem. Commun.* **1993**, *5*, 450 452. (b) Yamabe, S.; Kuwata, K.; Minato, T. Frontier-orbital analyses of ketene [2+ 2] cycloadditions. *Theor. Chem. Acc.* **1999**, *102*, 139 146.

(9) Wang, Y.; Wei, D.; Li, Z.; Zhu, Y.; Tang, M. DFT study on the mechanisms and diastereoselectivities of Lewis acid-promoted ketene alkene [2+ 2] cycloadditions: what is the role of Lewis acid in the ketene and C= X (X= O, CH2, and NH)[2+ 2] cycloaddition reactions? *J. Phys. Chem. A* **2014**, *118*, 4288 4300.

(10) (a) Cagnon, J.; Le Bideau, F.; Marchand-Brynaert, J.; Ghosez, L. Unusual regiochemistry of cycloaddition of ketenes to (R)-2-tert-butyldihydrooxazole derivatives. A simple route towards enantiomerically pure functionalised α-aminocyclobutanones. *Tetrahedron Lett.* **1997**, *38*, 2291 2294. (b) Ghosez, L.; Yang, G.; Cagnon, J. R.; Le Bideau, F.; Marchand-Brynaert, J. Synthesis of enantiomerically pure α-amino- -hydroxy-cyclobutanone derivatives and their transformations into polyfunctional three-and five-membered ring compounds. *Tetrahedron* **2004**, *60*, 7591 7606.

(11) (a) Tinant, B.; Declercq, J.-P.; Le Bideau, F.; Ghosez, L. Crystal structures of adducts of in situ generated phenylchloroketene to oxazoline (major isomer). *Bull. Soc. Chim. Belg.* **1997**, *106*, 233 234. (b) Tinant, B.; Declercq, J.-P.; Le Bideau, F.; Ghosez, L. Crystal structures of adducts of in situ generated phenylchloroketene to oxazoline (minor isomer). *Bull. Soc. Chim. Belg.* **1997**, *106*, 231 232.

(12) (a) Stucky, G.; Seebach, D. Substitutionen und Additionen an (R)-2-tert-Butyl- 4-1, 3-oxazolin-3-carbonsäure-methylester. *Chem. Ber.* **1989**, *122*, 2365 2375. (b) Seebach, D.; Stucky, G.; Pfammatter, E. Cycloadditionen an die Doppelbindung von (R)-2-tert-Butyl- 4-1, 3-oxazolin-3-carbonsäure-methylestern. *Chem. Ber.* **1989**, *122*, 2377 2389. (c) Seebach, D.; Stucky, G. Reactivity of (R)-2-tert-Butyldihydrooxazole Derivatives Prepared from Serine and Threonine: Novel, Versatile Chiral Building Blocks. *Angew. Chem. Int. Ed.* **1988**, *27*, 1351 1353. (d) Renaud, P.; Seebach, D. Preparation of Chiral Building Blocks from Amino Acids and Peptides via Electrolytic Decarboxylation and TiCl4-Induced Aminoalkylation. *Angew. Chem. Int. Ed.* **1986**, *25*, 843 844.

(13) Lamatsch, B.; Seebach, D.; Ha, T. K. Ab-initio-Studien an N-Acyliminium-Ionen. *Helv. Chim. Acta* **1992**, *75*, 1095 1110.

(14) Frisch, M.; Trucks, G.; Schlegel, H.; Scuseria, G.; Robb, M.; Cheeseman, J.; Scalmani, G.; Barone, V.; Petersson, G.; Nakatsuji, H. *Gaussian 16*; Gaussian, Inc.: Wallingford, CT, 2016.

(15) Hohenberg, P.; Kohn, W. Inhomogeneous electron gas. *Phys. Rev.* **1964**, *136*, No. B864.

(16) Chai, J.-D.; Head-Gordon, M. Long-range corrected hybrid density functionals with damped atom atom dispersion corrections. *Phys. Chem. Chem. Phys.* **2008**, *10*, 6615 6620.

(17) Marenich, A. V.; Cramer, C. J.; Truhlar, D. G. Supporting Information (PART I) Universal Solvation Model Based on Solute Electron Density and on a Continuum Model of the Solvent Defined by the Bulk Dielectric Constant and Atomic Surface Tensions Contents. *J. Phys. Chem. B* **2009**, *113*, 6378 6396.
(18) Luchini, G.; Alegre-Requena, J. V.; Funes-Ardoiz, I.; Paton, R. S. GoodVibes: automated thermochemistry for heterogeneous computational chemistry data. *F1000Research* **2020**, *9*, 291.
(19) Riplinger, C.; Sandhoefer, B.; Hansen, A.; Neese, F. Natural triple excitations in local coupled cluster calculations with pair natural orbitals. *J. Chem. Phys.* **2013**, *139*, No. 134101.
(20) Dunning, T. H., Jr. Gaussian basis sets for use in correlated molecular calculations. I. The atoms boron through neon and hydrogen. *J. Chem. Phys.* **1989**, *90*, 1007 1023.
(21) Neese, F. Software update: the ORCA program system, version 4.0. *WIREs Comput. Mol. Sci.* **2018**, *8*, No. e1327.
(22) (a) Lu, T.; Chen, F. Calculation of molecular orbital composition. *Acta Chim. Sin.* **2011**, *69*, 2393. (b) Lu, T.; Chen, F. Multiwfn: A multifunctional wavefunction analyzer. *J. Comput. Chem.* **2012**, *33*, 580 592.
(23) Legault, C. Y. *CYLview20*; Université de Sherbrooke, 2020.

https://doi.org/10.1021/acs.joc.2c00001
J Org Chem 2022 87 3613 3622